ADVANCES IN FOREST FIRE RESEARCH

2022

Edited by
DOMINGOS XAVIER VIEGAS
LUÍS MÁRIO RIBEIRO

Anatomy of the *Las Máquinas* wildfire using remote sensing tools

Jorge Valdivia[1]; Israel Avila[1]; Fernando Auat-Cheein[2]; Andrés Fuentes[2]; Pedro Reszka*[1]

[1]*Universidad Adolfo Ibáñez, Av. Diagonal Las Torres 2640, Peñalolén, Santiago, Chile*
{jorvaldivia@alumnos.uai.cl, jiavilaosses@gmail.com, pedro.reszka@uai.cl}
[2] *Universidad Técnica Federico Santa María, Avda. España 1680, Valparaíso, Chile*
{fernando.auat, andres.fuentes}@usm.cl

*Corresponding author

Abstract

The Las Máquinas wildfire took place in central Chile in the austral summer season of 2017 and became the most severe event in Chilean history, causing loss of life, property and the destruction of native forest, crops, large areas of commercial plantations and biodiverse habitats. Since this event has no precedent in Chilean wildfire history, it was used as an example to carry out a detailed analysis of the conditions before (pre-), during (per-) and after (post-) the fire from a remote sensing perspective. The goal of this work is to develop a framework to carry out detailed analyses of catastrophic fires for forensic and public policy purposes, making use of the advantages posed by Earth Observation satellites, including the simultaneous imaging of large areas with a good spatial resolution, and an ever-increasing temporal resolution, coupled with a sophisticated suite of instruments which allow measuring many parameters simultaneously. This study examines the biophysical, meteorological and physical variables like the evolution of the Normalized Difference Vegetation Index (NDVI), weather conditions, maximum temperature evolution, the Canadian Fire Weather Index (FWI), the burned area, the maximum fire radiative power, among others, for the five municipalities that were affected by the fire: Cauquenes, Chanco, Empedrado, Constitución and San Javier, all of which are located in the Maule Region. The results indicate that Las Máquinas wildfire took place under exceptional meteorological conditions. In particular, the conditions before the night when Santa Olga was destroyed were characterized by extreme values of the FWI, which caused a significant increase in the burned area and overwhelmed any response by the fire brigades.

1. Introduction

Central Chile experienced tragic wildfire events in the 2016-2017 season, which killed 11 people, destroyed over 1000 structures, including the complete destruction of the village of Santa Olga, burned down approximately one half of the protected forests of *Nothofagus alessandrii*, an endangered southern beech species endemic to Chile. The total burned area for the fires was of about 575,000 ha, with the damage occurring especially in the Maule Region (CONAF 2017, ONEMI 2017), which saw the destruction of ~10% of its total area. The *Las Máquinas* fire consumed 190,000 ha in a few days, becoming the most devastating event in Chilean history. This wildfire is analyzed in this paper solely relying on Earth Observation (EO) tools. The goal of this work is to develop a framework to carry out detailed analyses of catastrophic fires for forensic and public policy purposes, making use of the advantages given by EO satellites, including the observation of large tracts of landscapes with a good spatial resolution, and an ever-increasing temporal resolution, coupled with a sophisticated suite of instruments which allow measuring many parameters simultaneously. For this purpose, we analyzed the landscape conditions before the fire (*pre*-fire), the propagation of the fire front (*per*-fire) and the evolution of the vegetation in the years after the event (*post*-fire), using open-access satellite imagery obtained from multiple remote sensing instruments, giving a new perspective to the description of this event. Additionally, the *pre*- and *per*-fire Canadian Fire Weather Index (FWI) was calculated for the entire Region of Interest on a daily basis, based on remotely sensed data and physical simulations.

2. Methods & materials

2.1. Study area

The Maule region is located in Central Chile (35° 25' 36'' S, 71° 39' 79'' W), with an area of 30,296 km² (see Figure 1). The climate is prototypical Mediterranean. Forestry is one of the main economic activities, with large continuous *Pinus radiata* and *Eucalyptus globulus* plantations. The Region of Interest (ROI) corresponds to five municipalities within the Maule region, where the wildfire took place. These municipalities are: Cauquenes, Empedrado, San Javier, Chanco and Constitución, which correspond to the five zones shown in Figure 1 that are delimited by a thick black line filled with a gray hatched fill.
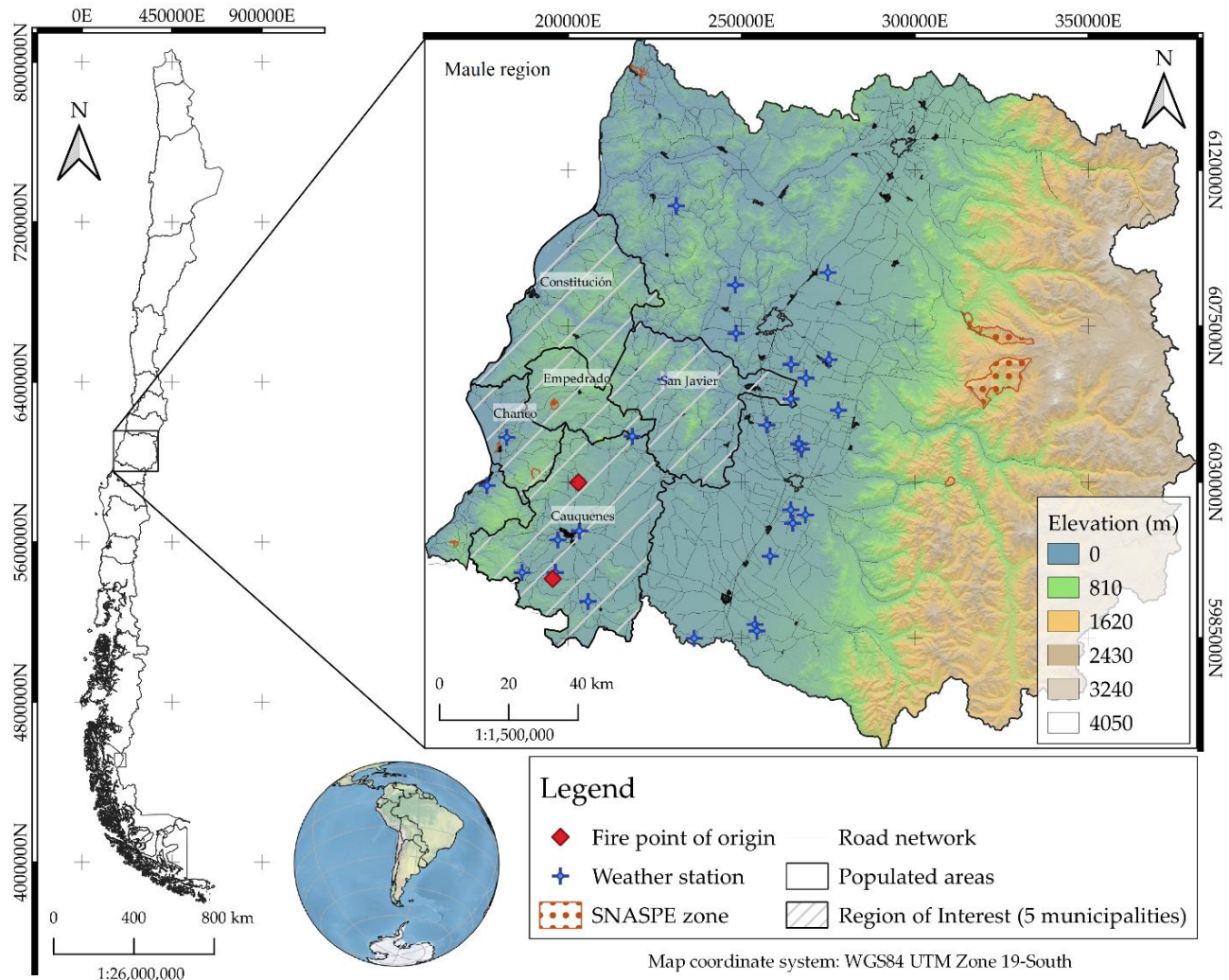
Figure 1. ROI with topography, weather stations, points of fire origins, and populated areas. SNASPE zones correspond to protected wilderness areas.

2.2. Burned area

Three different satellite products were used to calculate the burned area of the event: MODIS (product MCD64A1 v006 Burned Area (Giglio et al., 2015a), Landsat-8 pre- and post-fire images at Level-2 (surface reflectance with atmospheric correction), and Sentinel-2 pre- and post-fire images at Level-1C. The "sen2r" package (Ranghetti et al., 2020) was used in R to perform atmospheric, terrain and cirrus correction at the Top-Of-Atmosphere (TOA) for Sentinel-2 data, delivering Bottom-Of-Atmosphere (BOA) reflectance images. Landsat-8 and Sentinel-2 images were obtained from NASA's EarthExplorer. All images had < 0.5% cloud pixels within the ROI. Three images of Landsat-8 and Sentinel-2 were assembled to build the ROI, while only one MODIS Tile was required. The images were cropped and masked to the extent of the ROI. For Landsat-8 and Sentinel-2 BOA data, the following spectral indices were computed: Normalized Difference Vegetation Index (NDVI) (Rouse 1973), Normalized Difference Water Index (NDWI) (McFeeters 1996), Normalized Burn

Ratio (NBR) (Key & Benson 2006) and its temporal difference between pre, and post fire, i.e. the delta Normalized Burn Ratio (dNBR), which can represent the optimal separation of burned pixels from unburned ones and provide an scaled index representing the burn severity (Van Wagtendonk 2004). The two following filters were applied to the data: (i) NDVI pre-fire must be greater than 0.25, and (ii) NDWI must be lower than zero, meaning that only vegetation (El-Gammal et al., 2014) and non-water pixels can burn. Several threshold values for the dNBR were studied.

2.3. Vegetation evolution

Using MODIS product MOD13A1 (Vegetation indices 16-Day) (Didan 2015), the NDVI (Rouse 1973) was calculated. The average NDVI value for each municipality was computed from January 2010 to January 2022.

2.4. Fire weather

2.4.1. Standardized precipitation index

The Standardized Precipitation Index (SPI) (McKee et al., 1993) is based on the deviation of rainfall from normal data, and is computed by summing precipitations over k months, and fitting these accumulated precipitation values to a parametric statistical distribution from which probabilities are transformed to the standard normal distribution ($\mu = 0$, $\sigma = 1$). The precipitation data corresponded to the Integrated Multi-satellitE Retrievals for Global Precipitation Measurements (IMERG-GPM) monthly accumulated precipitation data product (GPM 3IMERGM.06) at a 0.1 degree × 0.1 degree spatial resolution (Huffman et al., 2019a), acquiring monthly accumulated precipitations from January 2001 to January 2016. SPI was computed using the "SPEI" package (Beguería & Vicente-Serrano 2017) in R, based on the Pearson Type III distribution, i.e. 3-parameter Gamma distribution function (Guttman 1999). In addition, the area under the curve (AUC) of the SPI was also studied.

2.4.2. Temperature evolution

Temperature evolution was carried out using the maximum monthly temperature from 1979 to 2019 grid product of Chile's CR[2]. The product was built using statistical regionalization of the ERA-Interim atmospheric reanalysis data, while adding local information (such as topography and temperature observations) and surface temperature estimates by MODIS Land Surface Temperature product (M*D11A1) (Wan et al., 2015). The raster pixel-data was extracted for the whole ROI and then the average value was computed and stored.

2.4.3. FWI

The FWI was calculated using remote sensing products and physical simulations. $FWI = f(T_a, U_r, PP, RH)$, where T_a is the ambient temperature or NSAT (near-surface air temperature, in °C), U_r is the wind speed at 10 m height (km/h), PP is the precipitation (mm), and RH is the relative humidity (%). Wind speed was simulated using WindNinja V3.6.0 (Forthofer et al., 2014), with a landscape file for the ROI built by using primarily the information of the National Land Use Inventory (LUI) (CONAF 2016). NSAT was calculated using multiple linear regression models and machine learning random forests regression algorithms. The variables used are those proposed by Zhang et al., 2014. The regression training dataset was built by using daily images of NDVI, PW (precipitable water vapor, cm) and T_s (land surface temperature) from 2010 to 2016 for the month of January only. The pixels at the location of the weather stations within the ROI were extracted, as well as the air temperature measured by the weather station at the closest acquisition time of the satellite-product.

Precipitation was obtained from the IMERG-GPM (Huffman et al., 2019b), where the product GPM IMERG Final Precipitation L3 Daily at a 0.1 degree × 0.1 degree spatial resolution was used. Relative humidity was obtained by calculating the quotient of the actual vapor pressure, e_a, and the saturation vapor pressure, $e°(T_a)$. The only variables required are the near-surface air temperature (NSAT) and the dew-point temperature (T_{dew}) (Allen et al., 1998; Lawrence 2005). The latter was obtained from MODIS M*D07 product (atmospheric profiles) (Borbas et al., 2016). Finally, the FWI was computed in R using the "cffdrs" package (Wang et al., 2017) with adjusted latitude and initial conditions of the Fine Fuel Moisture Code (FFMC), Duff Moisture Code (DMC) and Drought Code (DC) derived from the fire danger indices historical data from the Copernicus Emergency Management Service (Vitolo et al., 2019).

3. Results

3.1. Burned area

Landsat-8 and Sentinel-2 burned area for several dNBR threshold values is shown in Figure 2. The upper bound of the red rectangle corresponds to the burned area reported by the authorities (218,076 ha), while the lower bound corresponds to the burned area calculated by means of the MODIS MCD64A1 product. Figure 3 shows the burned area obtained from MODIS, and both Landsat-8 and Sentinel-2 for certain dNBR threshold values. Figure 4 exhibit the evolution of the daily burned area.
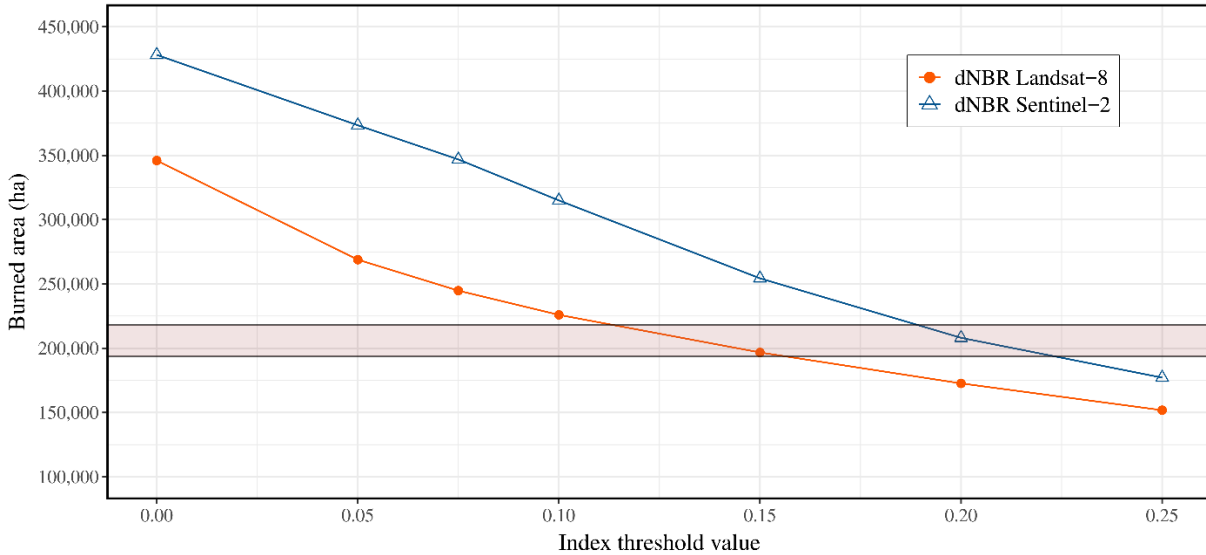
Figure 2. Burned area versus dNBR threshold values for Landsat-8 and Sentinel-2 images.
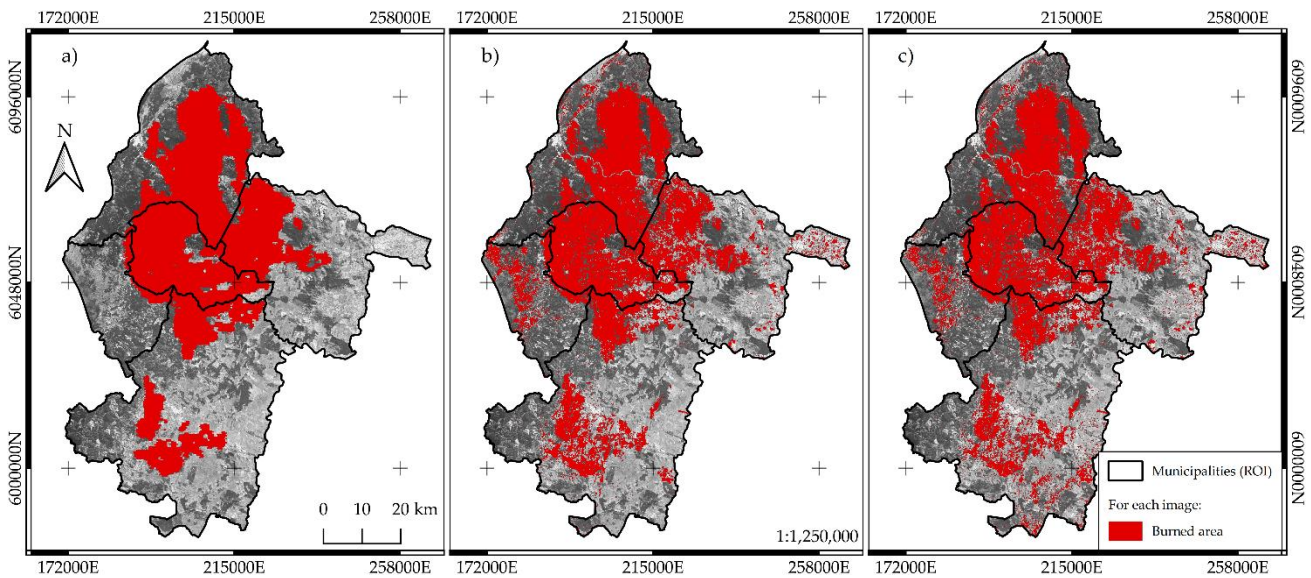
Figure 3. Burned area for a) MODIS MCD64A1 product, b) Landsat-8 with dNBR=0.135, and c) Sentinel-2 with dNBR=0.205. Considering the dNBR threshold values mentioned before, the Landsat-8 and Sentinel-2 burned area results were 204,440 ha and 204,450 ha, respectively. While the affected surface with MODIS MCD64A1 was 193,804 ha. Map coordinate system is WGS84 UTM Zone 19-South.
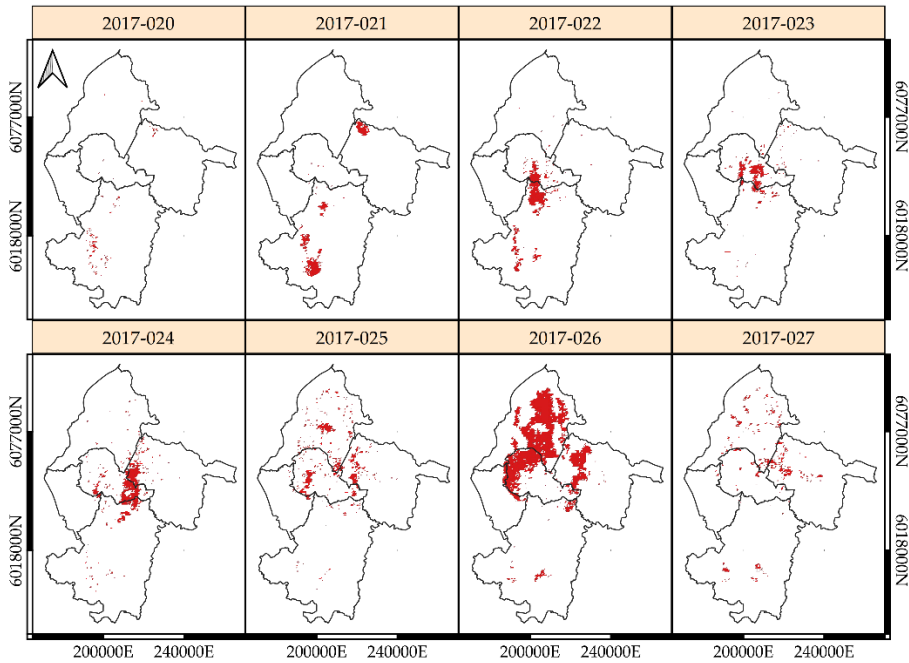
Figure 4. Burned area evolution (MODIS MCD64A1 product) between Julian days 020 – 027 (January 20th to January 27th, 2017) within the ROI. Each image corresponds to daily data.

3.2. Vegetation evolution

The results in Figure 5 shows that the most affected municipality within the ROI in terms of its flora was Empedrado. Note that around 89% of Empedrado surface-area was burned.
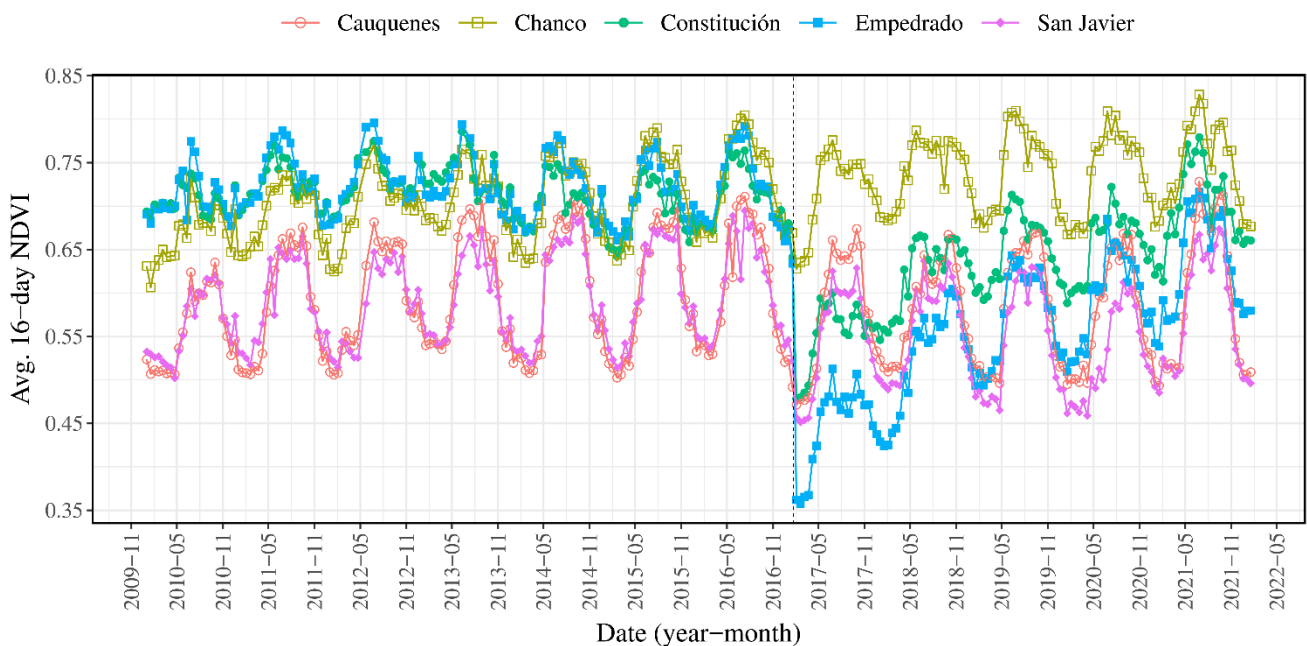
Figure 5. Average NDVI evolution from January 2010 to January 2022 for each municipality within the ROI. The vertical dashed line corresponds to the fire start date (January 20, 2017).

3.3. Standardized precipitation index

Severe drought values were found the year prior to the event (see Figure 6a). Furthermore, the downward trend displayed by the cumulative SPI AUC in Figure 6b corresponds to a persistent drought from 2009 onwards.
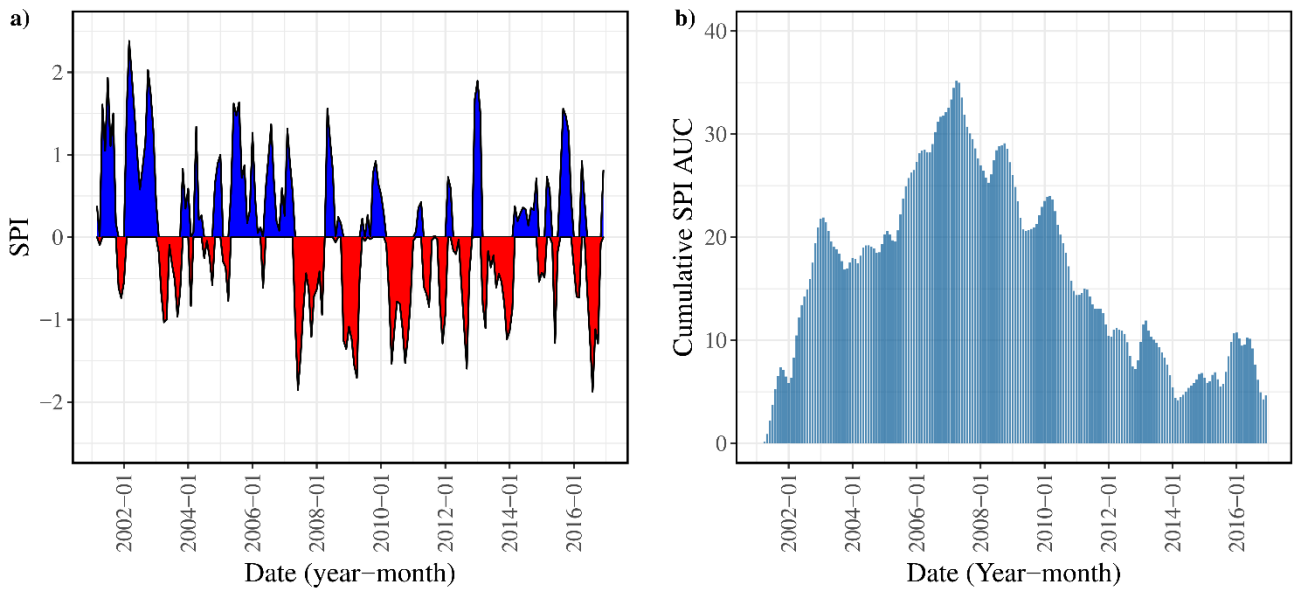
Figure 6. Standardized precipitation index (SPI) a) evolution and b) AUC analysis within the ROI from 2001 to 2016.

3.4. Temperature evolution

Record temperature of around 29°C were found on December 2016, the month prior to the event and the highest since 1979 within the ROI.
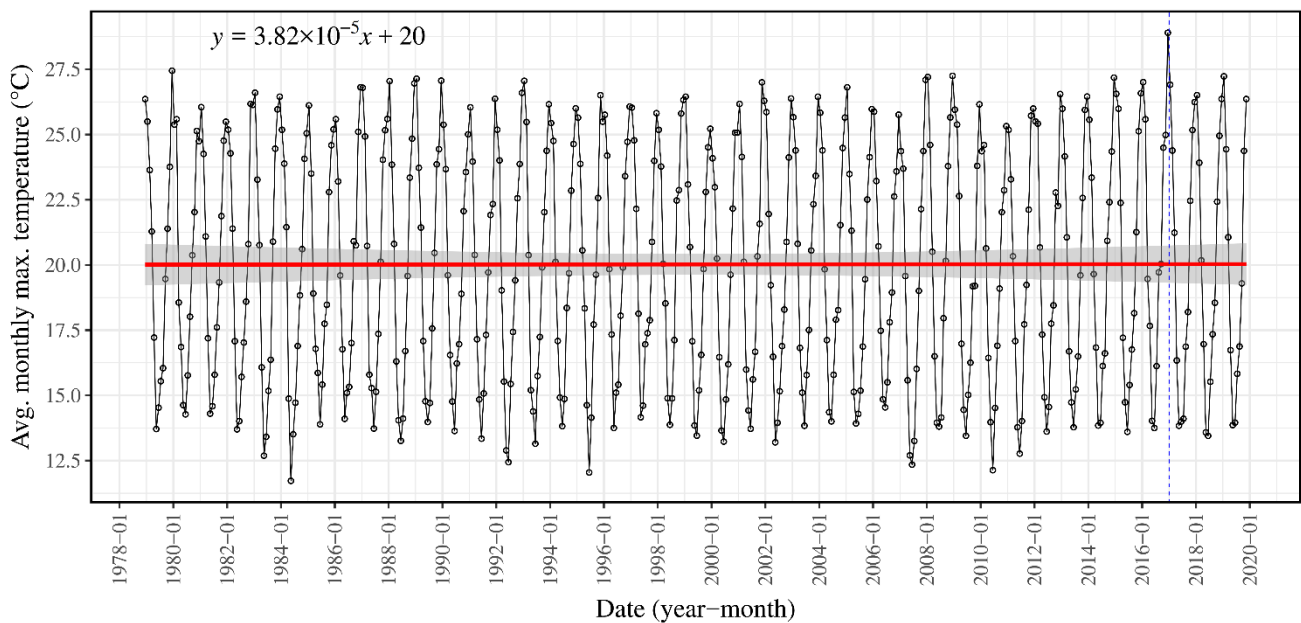
Figure 7. Average maximum temperature within the ROI from January 1979 to December 2019. Red line corresponds to the data trendline, the gray zone is the confidence interval, and the vertical dashed line is the fire start date.

3.5. Canadian FWI

FWI evolution and validation are shown in Figure 8. All datasets exhibit an increase in the FWI during the event (Figure 8a, 8c and 8e). On the other hand, a FWI map is shown in Figure 9. As it is possible to observe, on January 24th, Aqua FWI values at the north of the ROI exhibit extreme FWI values of 52.4±5.5, which is a day prior to the catastrophic events that destroyed the village of Santa Olga.
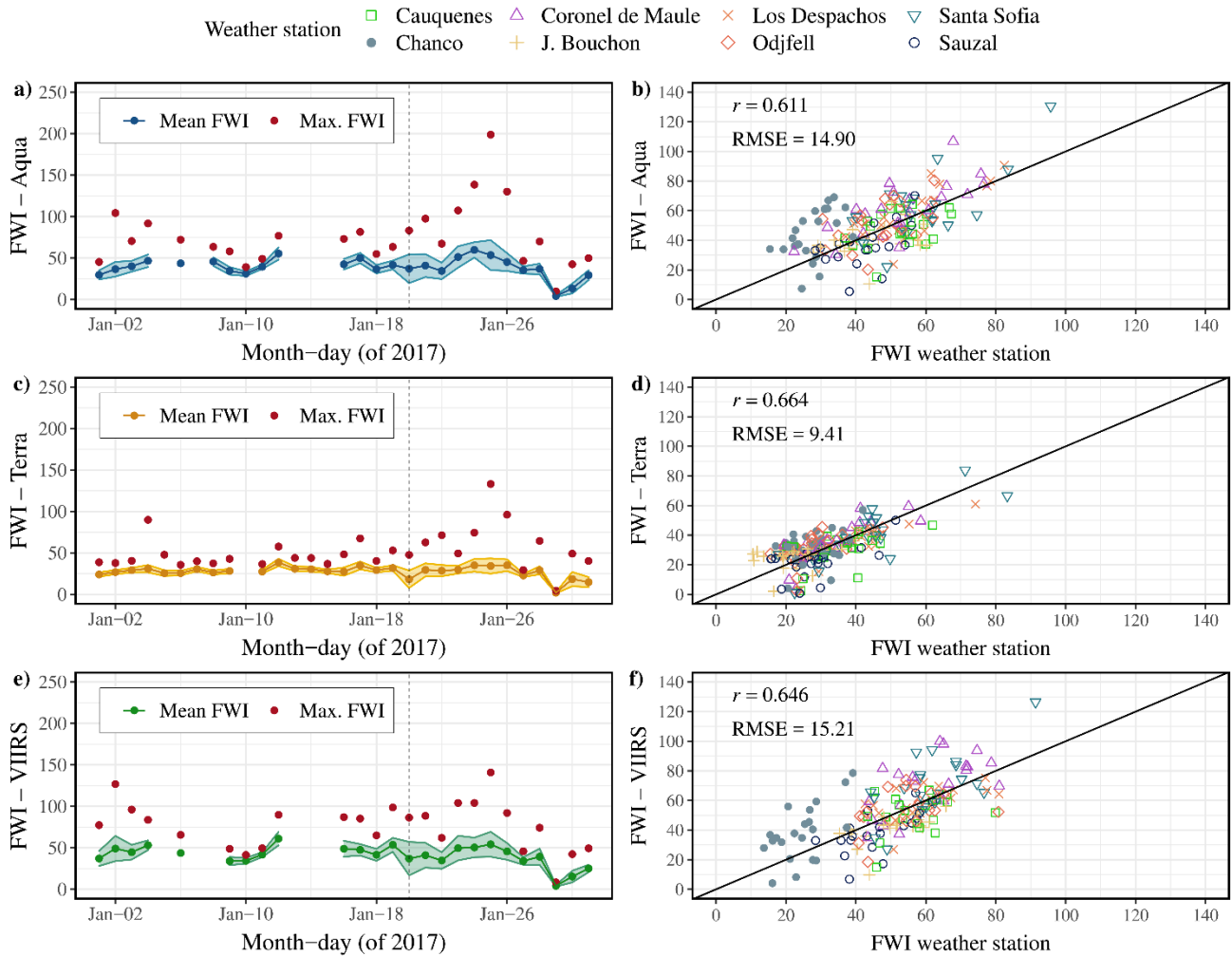
Figure 8. Canadian FWI evolution for a) Aqua, c) Terra and e) VIIRS-SNPP, and validation for b) Aqua, d) Terra, and f) VIIRS-SNPP. The colored areas in a), c) and e) represent the standard deviation of the FWI. The vertical dashed line corresponds to the fire start date.
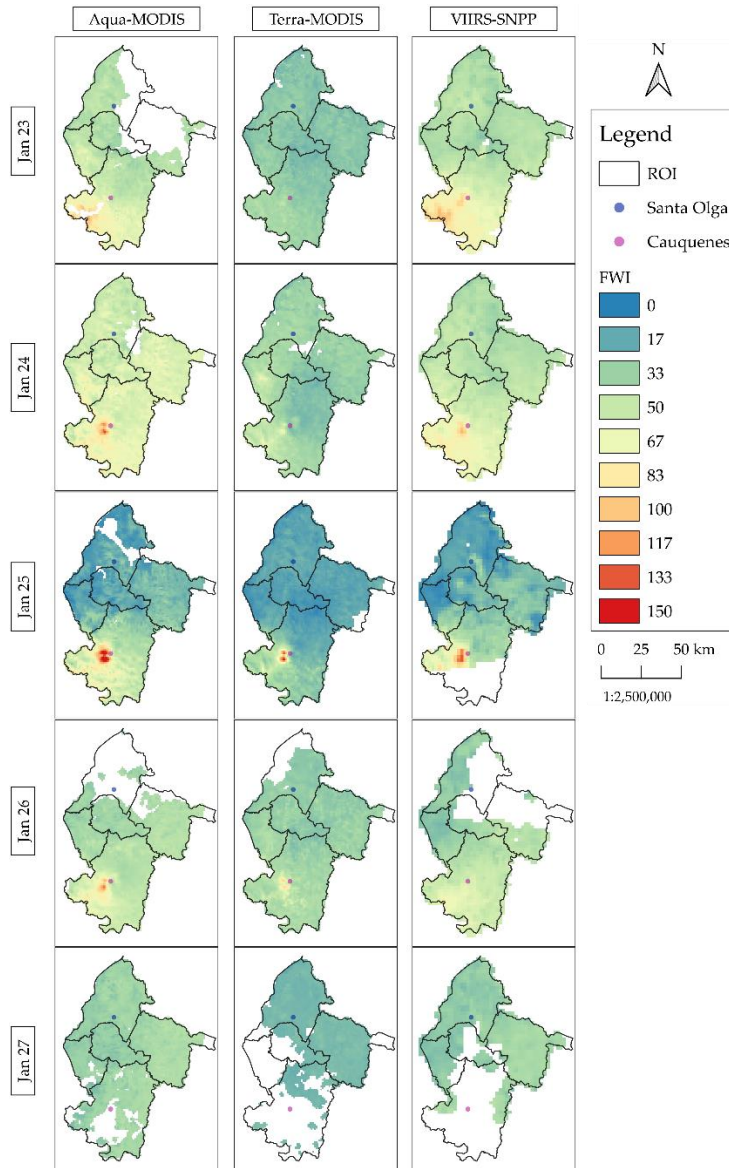
Figure 9. Canadian FWI estimated with Aqua-MODIS, Terra-MODIS, and VIIRS-SNPP, from January 23 to 27, 2017.

4. Conclusion

The *Las Máquinas* wildfire took place under exceptional meteorological conditions. The lowest NDVI values were registered for Empedrado during the event. On the night of January 25, the wildfire propagated at a peak rate, particularly among Empedrado (center), Constitución (north) and San Javier (east) (Fig. 4). The SPI data shows a consistent moderate-to-severe drought in the ROI, in agreement with the mega-drought observed in central Chile (Garreaud et al., 2020). The fire also occurred in a period with a record averaged maximum temperature (Fig. 7).

FWI results show that the index can be calculated on a daily basis from remotely sensed data (and wind-speed simulations), and that a day prior to the catastrophic events in Santa Olga, extreme FWI values were observed within the Constitución municipality. Moreover, the pre-fire FWI trend analysis (from January 1 to 19) showed positive slope values, which might be an indicator of wildfire risk.

From the FWI validation results, it is possible to conclude that the use and application of a remote sensing methodology to calculate the FWI is feasible, since the results were neither strongly overestimated nor underestimated.

Through remote sensing, we were able to compile a large amount of open-access satellite-based information with a good spatial and temporal resolution. This detailed information, and the reported framework for retrieving and processing the data, can contribute to the forensic study of large wildfires, particularly those occurring in remote areas or countries without a sophisticated wildfire safety and response infrastructure.

5. Acknowledgements

6. Bibliography

Allen, R. G., Pereira, L. S., Raes, D., & Smith, M. (1998). Crop evapotranspiration-Guidelines for computing crop water requirements – FAO Irrigation and drainage paper 56. FAO, Rome, 300(9), D05109.

Beguería, S. & Vicente-Serrano, S. M. (2017). SPEI: Calculation of the Standardized Precipitation-Evapotranspiration Index. R package version 1.7.

Borbas, E. E., Seemann, S., Li, Z., Li, J., Kern, A., & Menzel, W. P. (2016). MODIS Atmosphere Profiles Product (07_L2). NASA MODIS Adaptive Processing System. Goddard Space Flight Center.

CONAF (2016). Catastro de uso de suelo y vegetación. Comisión Nacional Forestal. Obtained in March 2022 from Infraestructura de Datos Espaciales (IDE).

CONAF (2017). Análisis de la afectación y severidad de los incendios forestales ocurridos en enero y febrero de 2017 sobre los usos de suelo y los ecosistemas naturales presentes entre las regiones de coquimbo y los ríos de chile. Corporación Nacional Forestal, Informe Técnico. 56 p. Santiago, Chile.

Didan, K., Huete, A. (2015). MOD13A1 MODIS/Terra Vegetation Indices 16-Day L3 Global 500m SIN Grid. NASA LP DAAC.

El-Gammal, M.; Ali, R.; Samra, R., *J Am Sci.* 2014, 10, 108–113.

Forthofer, J. M., Butler, B. W., & Wagenbrenner, N. S., *Int. J. Wildland Fire* 2014, 23(7), 969-981.

Garreaud, R. D., Boisier, J. P., Rondanelli, R., Montecinos, A., Sepúlveda, H. H., Veloso-Aguila, D., *Int J Climatol* 2020, 40(1), 421-439.

Giglio, L., Justice, C., Boschetti, L., Roy, D. (2015a). MCD64A1 MODIS/Terra+ Aqua Burned Area Monthly L3 Global 500 m SIN Grid V006 Burned Monthly 500m. NASA EOSDIS Land Processes DAAC: Sioux Falls, SD, USA.

Guttman, N. B., *J Am Water Resour As* 1999, 35(2), 311-322.

Huffman, G.J., E.F. Stocker, D.T. Bolvin, E.J. Nelkin, Jackson Tan (2019a), GPM IMERG Final Precipitation L3 1 month 0.1 degree x 0.1 degree V06, Greenbelt, MD, Goddard Earth Sciences Data and Information Services Center (GES DISC).

Huffman, G.J., E.F. Stocker, D.T. Bolvin, E.J. Nelkin, Jackson Tan (2019b), GPM IMERG Final Precipitation L3 1 month 0.1 degree x 0.1 degree V06, Greenbelt, MD, Goddard Earth Sciences Data and Information Services Center (GES DISC)

Key, C.H.; Benson, N.C. Landscape assessment (LA) – Sampling and analysis methods. Technical Report RMRS-GTR-164-CD, USDA Forest Service, 2006.

Lawrence, M.G., *B. Am. Meteorol. Soc*. 2005, 86, 225–234.

McFeeters, S.K., *Int J Remote Sens* 1996. 17, 1425–1432.

McKee, T. B., Doesken, N. J., & Kleist, J., In *Proceedings of the 8th Conference on Applied Climatology* 1993 17(22), 179-183.

ONEMI (2017). Monitoreo para la Región del Maule por incendios forestales. Oficina Nacional de Emergencia del Ministerio del Interior, Gobierno de Chile. https://www.onemi.gov.cl/alerta/monitoreo-para-la-region-del-maule-por-incendios-forestales/.

Rouse, J.W.; Haas, R.H.; Schell, J.A.; Deering, D.W.; Harlan, J.C. Monitoring the vernal advancement and retrogradation (greenwave effect) of natural vegetation. Technical Report E74-10676, Texas A&M University, Remote Sensing Center, College Station, Texas, United States. Prepared for Goddard Space Flight Center, 1973.

Ranghetti, L., Boschetti, M., Nutini, F., Busetto, L *Comp Geosci* 2020. 139, 104473.

Van Wagtendonk, J.W., Root, R.R. and Key, C.H., *Remote Sens Environ* 2004, 92(3), 397-408.

Wan, Z., Hook, S., Hulley, G. (2015). MOD11A1 MODIS/Terra Land Surface Temperature/Emissivity Daily L3 Global 1km SIN Grid V006. NASA EOSDIS Land Processes DAAC.

Wang, X., Wotton, B. M., Cantin, A., Parisien, M-A., Anderson, K., Moore, B., Flannigan, M. D., *Ecol Proc*ess 2017, 6(1), 5.

Zhang, H., Wu, B., Yan, N., Zhu, W., & Feng, X., *J Geophys Res-Atmos* 2014, 119(21), 12-256.